Eur Biophys J (1991) 19:241–251

European Biophysics Journal

The reaction cycle of bacteriorhodopsin: an analysis using visible absorption, photocurrent and infrared techniques

K.-H. Müller [1], H. J. Butt [2], E. Bamberg [2], K. Fendler [2], B. Hess [1], F. Siebert [2,3], and M. Engelhard [1]

[1] Max-Planck-Institut für Ernährungsphysiologie, Rheinlanddamm 201, W-4600 Dortmund, Federal Republic of Germany
[2] Max- Planck-Institut für Biophysik, Kennedyallee 70, W-6000 Frankfurt 70, Federal Republic of Germany
[3] Institut für Biophysik und Strahlenbiologie der Universität, Albertstrasse 23, W-7800 Freiburg, Federal Republic of Germany

Received June 27, 1990/Accepted in revised form December 7, 1990

Abstract. The light activated absorbance changes and photo-electric events of bacteriorhodopsin (bR) were simultaneously measured. The results were compared with the kinetics of the time resolved infrared signals which are characteristic for protonation changes of Asp residues, chromophore vibrations, and amide I vibrations. Each data set was analyzed separately. Assuming first order reactions the experimental curves in the time range from *L* back to bR could be fitted by a sum of five exponentials. However, for the photocurrent signal only four exponentials were necessary. The corresponding half-life times were of the same order of magnitude. Simultaneous fits of the traces from absorption changes in the visible range and the photocurrent signal provided evidence that the photocurrent data could also be described by the same sum of exponentials as the data obtained in the visible range. The rate constants obtained from the different methods applied were, within the limits of error, identical. These results demonstrate that retinal monitors not only charge displacements but also conformational movements of the protein moiety. The reprotonation of the Schiff base occurs synchronously with a protonation change of an internal aspartic acid which absorbs at 1755 cm^{-1}. From the IR-signals, amplitude spectra could be derived which provided evidence that Asp-residues absorbing at 1765 cm^{-1} (Asp85) and 1755 cm^{-1} are still protonated in the *O*-intermediate. Major conformational changes of the peptide back bone occur in the time range of the $L \rightarrow M$ transition and with opposite sign during the decay of the *O*-intermediate.

Key words: Bacteriorhodopsin – Photocycle – Time resolved infrared spectroscopy – Photocurrent

Introduction

The light activated photocycle of bacteriorhodopsin, the only protein of the purple membrane from *Halobacterium halobium*, has been the subject of extensive research (for recent reviews see Hess et al. 1982; Stoeckenius and Bogomolni 1982; Ovchinnikov et al. 1982; Oesterhelt and Tittor 1989). It is now well established that after the excitation of the chromophore by light the system relaxes thermally back to the original state via several intermediates. These intermediates are characterized by their absorption maxima, the isomerization of the retinal chromophore, the protonation state of the Schiff base linkage to the protein, and the protonation state of internal Asp residues. The first part of the photocycle, which includes the deprotonation of the Schiff base and the ejection of a proton to the extracellular side of the membrane, is completed in the μs range. In the second part, which covers approximately 50 ms, a proton is regained from the cytoplasm and the Schiff base is reprotonated. From the data gained from the analysis of the absorption changes in the visible range (e.g. Oesterhelt and Hess 1973; Lozier et al. 1975; Xie et al. 1987; Kouyama et al. 1988; Polland et al. 1986) it was concluded that after reaching the first ground state-intermediate, which was named *J*-, *K*-, *L*-, *M*-, *N*-, and *O*-intermediates could be discerned.

However, it is not yet established whether these intermediates follow each other in an unidirectional path or if back-reactions, branching of the photocycle, and/or different bR species exist (see for example Nagle et al. 1982; Parodi et al. 1984; Váró and Lanyi 1990 and literature therein).

Recently, the discussion of the mechanism of the photocycle was resumed and several different kinetic models were proposed. From the kinetic behavior of the bR at high pH (Dancsházy et al. 1986) or low temperature and high salt conditions (Drachev et al. 1986) the presence of an intermediate was deduced which was placed between *M* and bR. This intermediate turned out to be identical to the *N*-intermediate which was first described by Lozier et al. 1975, Kouyama et al. 1988; Fodor et al. 1988). Additionally, back-reactions were considered which were placed in the last part of the photoreaction cycle (Kouyama et al. 1988, Fodor et al. 1988). Similar conclusions were drawn by Chernavskii et al. (1989) from temperature

Offprint requests to: M. Engelhard

pulse experiments which indicated that the back-reactions from N to M and O to N cannot be neglected (see also Váró and Lanyi 1990; Váró et al. 1990; Ames and Mathies 1990). Additionally, a possible branching of the photocycle was discussed. In a new study using temperature jump experiments Butt et al. (1989a) concluded that the branching point must be placed before the L-intermediate. Diller and Stockburger (1988) observed, in kinetic resonance Raman measurements, a long lived intermediate with the spectroscopic properties of L. They concluded that this intermediate must originate from a bR species which is different from the bR giving rise to M.

The question about the nature and the number of intermediates and the exact sequence of spectroscopic events during the photocycle is of importance because these data are the presupposition for understanding the molecular mechanism of the intramolecular transfer of the proton.

Further insight into the photo-reaction cycle can be expected from the analysis of absorption changes of infrared signals and photoinduced electrical signals. The normal mode vibrations can very often be assigned to characteristic molecular groups, e.g. carbonyls of carboxylic acids, the C=C double bonds of the retinal chromophore or the amide of the peptide bond. For bacteriorhodopsin, it has been shown by time resolved infrared measurements and static FTIR difference spectroscopy that during the photocycle internal carboxyl-groups undergo protonation-deprotonation reactions (Rothschild et al. 1981; Bagley et al. 1982; Siebert et al. 1982) which were assigned to Asp-residues (Engelhard et al. 1985; Eisenstein et al. 1987). In recent experiments using mutant bR's from site directed mutagenesis (Braiman et al. 1988; Mogi et al. 1988) and single site mutants in their natural environment (Soppa and Oesterhelt 1989) the protonation changes of the carboxyl-groups could be assigned to specific Asp residues. Furthermore, it could be verified that they are participating in the proton transfer (Braiman et al. 1988; Butt et al. 1989b; Tittor et al. 1989; Otto et al. 1989; Stern et al. 1989; Gerwert et al. 1989; Gerwert et al. 1990).

In further measurements the kinetics of the photoinduced electrical signals of oriented purple membranes have been analyzed (e.g. Herrmann and Rayfield 1976; Drachev et al. 1978; Fahr et al. 1981; Trissl 1985; Keszthelyi 1987). These experiments revealed rate constants which were tentatively correlated with the formation and decay of the photocycle intermediates.

Only a few experiments have so far been described which rely on more than one method. For example, similar kinetics were observed in photocurrent and visible absorbance changes (Drachev et al. 1978; Drachev et al. 1984; Keszthelyi and Ormos 1980; Dér et al. 1985). In another investigation Trissl (1985) could not correlate unequivocally the fast electrical events with the spectroscopically detected $K \rightarrow L$ and $L \rightarrow M$ transitions.

To obtain a consistent picture of the molecular events involved in the intramolecular proton transfer, three different techniques were applied in the investigation presented here: Absorption measurements in the visible and the infrared region were combined with electrical data. The visible absorbance changes were measured simultaneously with the photocurrent. The infrared data were collected separately from the visible events but on the same sample and under the same temperature and ionic conditions. This allows direct comparison of the data obtained by the different methods which is important if questions such as the coupling of spectroscopic events, protein movement and charge transport are to be addressed. In addition, the methods supplement each other and intermediates which do not appear in one technique might be discernible in another.

Materials and methods

All reagents used were reagent grade. Purple membrane fragments were prepared from *Halobacterium halobium* strain S9 (Oesterhelt and Stoeckenius 1974). The samples were photolyzed by a saturating laser flash from a YAG laser (Quantel, France) using a wavelength of 532 nm. For the infrared measurements an Excimer Laser pumped-dye laser-system (3 mJ) (Lambda Physik) was used.

After a preamplification stage which was different for the different techniques, the time resolved IR, absorption, and photocurrent signals were recorded and averaged by a home built transient recorder with a combined linear and logarithmic time base. Reactions could be observed from μs to 1 s with a time resolution of 0.2 μs.

After amplification by a DC-coupled preamplifier, a fast 8-bit AD-conversion is applied. In the LOG-mode a measuring trace has 512 data points and is divided into three parts, a linear pretrigger, a fast linear dwell time of 128 data points, and the logarithmic part. In the two linear parts the sweep time per point can be varied from 0.2 μs up to 2000 μs in five steps. The logarithmic part starts with a decade of 2 μs per point. In the second decade, two data points are averaged before being stored, in the third four data points, and so on. In the n^{th} decade 2^{n-1} data points are averaged so that the quality of the data becomes better in each decade. The number of points of the logarithmic part is restricted to 207 data points which provides for a maximum measuring time of about two and half minutes. The time range of a single measurement can cover more than eight orders of magnitude and measurements can be done either in single mode or averaged over up to 4096 sweeps. Statistical weights were calculated from the empirical variance of the data points as described in detail (Müller and Plesser 1991).

Infrared- and visible absorption measurements on hydrated purple membrane films

The time resolved infrared spectra were obtained on a Perkin-Elmer infrared spectrophotometer, model PE 180, modified according to Mäntele et al. (1982). For the infrared measurements a purple membrane suspension in distilled water was dried on a CaF_2 window as described in Mäntele et al. (1982). The IR-signals were recorded at 1800 cm^{-1}, 1770 cm^{-1}, 1765 cm^{-1}, 1760 cm^{-1}. From

1755 cm^{-1} to 1727 cm^{-1} every 3rd wavenumber was taken. Additionally, the amide vibrations at 1610 cm^{-1} and 1660 cm^{-1} and the chromophore vibrations at 1510 cm^{-1} and 1525 cm^{-1} were chosen. Two separate sets of experiments with 8×128 averages were performed. The two sets of measurements were normalized to each other using the signal at 1525 cm^{-1}. All experiments were done at 293 K with the actual temperature at the hydrated film within the cuvette being slightly higher (max. 1.5 K).

Directly before and after the infrared measurements the absorbance changes in the visible range were followed at 650 nm, 600 nm, 570 nm, 500 nm, and 415 nm. For these experiments the cuvette had to be taken from the infrared sample holder and placed in a separate thermostatted (293 K) unit to measure the photocycle at the wavelength given above.

Electrical- and visible-absorbance measurements on gels containing purple membrane

For the photocurrent measurements the purple membranes were fixed and oriented in polyacrylamide gel according to Eisenbach et al. (1977) and Dér et al. (1985), with final concentrations of 11% acrylamide, 0.3% N · N′-methylene *bis*-acrylamide, 0.15% ammonium persulfate, 1% tetramethylethylenediamine and 15 μ*M* bacteriorhodopsin. Pieces ($1.3 \times 7 \times 7$ mm^3) were cut from the gel and washed for 3 days in electrolyte. It was always ensured that bacteriorhodopsin was light-adapted.

For the measurements, the gel (after incubation in phosphate buffer, 25 m*M*, pH 6.88 for 2 h) was placed in the middle of a 1.3 mm thick cuvette and filled with electrolyte. Platinized platinum or silver chloride electrodes, screened from direct light, were immersed on both sides of the gel. The cuvette was shielded in a thermostatically regulated (293 K) Faraday-cage which contained two windows of 7×7 mm^2 for the excitation and measuring light. To check the electrode behavior, step voltages of ±1 mV, ±10 mV and ±100 mV were applied in series to the cuvette and the resulting current was observed. The current could be described by two exponentials of 5 s and 70 s (Pt/Pt electrodes) or 8 s and 300 s (Ag/AgCl electrodes), reflecting electrode capacitance and diffusion polarization. A home made current amplifier with a time resolution of 1 μs was connected to the electrodes.

The absorbance changes were simultaneously observed with a photomultiplier placed directly behind the gel at wavelengths of 650 nm, 600 nm, 570 nm, 500 nm and 415 nm.

Time resolution of the absorption and current measurements

Although the transient recorder had a time resolution of 0.2 μs, measurements of half-lives shorter than 3 μs are not reliable. The time resolution of the photocurrent measurements was determined by the response time of the current amplifier which had a resolution of 1 μs. In the case of the absorption measurements the scatterd laser flash causes a strong artifact at times smaller than 3 μs. For the data evaluation this early time had to be taken into account. Therefore, the data were not omitted in figures and tables. However, it should be emphasized, that only components with half lifes greater than 3 μs can be measured accurately.

Results

A. Determination of kinetic parameters

Absorption changes in the visible range and photocurrent. Bacteriorhodopsin which was imbedded in a polyacrylamide gel was excited by a saturating laser flash. Figure 1 shows the spectral shifts during the photocycle on a logarithmic time scale measured at five different wavelengths. These are characteristic for the depletion and reformation of bR and for formation and decay of the intermediates of the photocycle. The scattered laser flash causes a strong artifact at the beginning of the trace. Therefore, the optical data can only be reliably evaluated beyond times > 3 μs.

In the range from 10 μs to 1 ms two rate constants can be found with half times of $\tau_2 = 70$ μs and $\tau_3 = 370$ μs. τ_2 is in the time range of the *L* to *M* transition, whereas for τ_3 no direct correlation to the photocycle intermediates can be given. In the time range between one and five milliseconds two clearly distinct rate constants τ_4 and τ_5 belonging to the *M*- and the *O*-intermediates are found.

Simultaneously with these measurements, the photocurrent $I(t)$ was recorded, the time course of which is shown in Fig. 2 on a logarithmic time scale ranging from 0.2 μs to 100 ms. The last part of the photocurrent signal is presented with different magnification to emphasize the negative amplitude of τ_6. The negative peak at the beginning is a convolution of the response function of the measuring unit, which has a rise-time of some hundred nanoseconds, and the photoelectric signal generated by the purple membrane. Therefore, the evaluation for time periods shorter than 3 μs is unreliable.

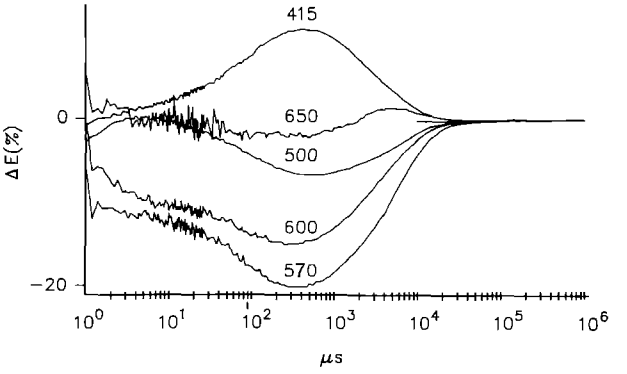

Fig. 1. Time course of absorbance changes of bR after excitation measured at 415 nm (415), 500 nm (500), 570 nm (570), 600 nm (600), and 650 nm (650). bR was imbedded in a polyacrylamide-gel. For experimental details see Materials and methods

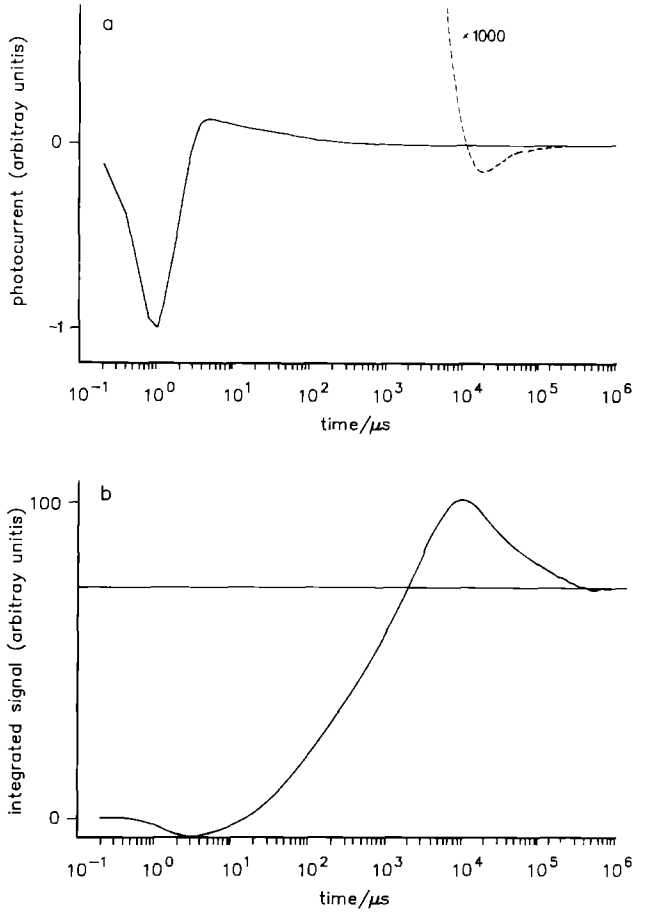

Fig. 2a, b. Photoelectric response of bR after light excitation. **a** photocurrent signal; the broken line is a 1000 fold magnification of the original signal. **b** Integration of the signal in **a**. Same sample as in Fig. 1

Table 1. Half-lives of the six first order rate constants (in μs). The data were fitted using the absorption changes in the infrared (IR) and from the same sample in the visible range (Vis_{IR}). Similarly, the kinetic data from bacteriorhodopsin immobilized in gels were derived using the absorption changes (Vis_{El}) and photocurrent (El). In the last column (Vis + El) the data from a simultaneous fit of photocurrent and absorption changes in the visible range are given. The numbers in parenthesis correspond to the numbering of the rate constants by Xie et al. (1987). The time constants for $i=1$ are determined by a superimposition of the physiological signals and artifacts from the measuring units (see text)

i	Vis_{IR}	IR	Vis_{El}	El	Vis + El
1* (1)	1.3	1.5	2	2	2
2 (5)	39	40	70	58	61
3 (7)	250	180*	370	300	350
4 (4)	1 150	1 530	1 720	–	1 400
5 (3)	3 950	5 150	3 500	3 150	3 600
6* (6)	–	23 000	13 000	9 200	11 000

* Significant, large standard deviation

Table 2. Apparent amplitudes (A) corresponding to the six rate constants of the photocurrent (Vis + El) and the amide stretching vibration at 1660 cm^{-1}. The amplitudes of the photocurrent were derived from the combined fit of electrical signal (El) and the absorption changes in the visible range (Vis)

	Vis + El		IR (1660 cm^{-1})	
i	$\tau_{1/2}$	A	$\tau_{1/2}$	A
2	61	20±3	31	0.46±0.04
3	350	13±4	250	0.03±0.02
4	1400	11±5	1150	−0.12±0.02
5	3600	56±5	3950	−1.12±0.02

Figure 2b shows the integral of the photocurrent, which is proportional to the charge movement parallel to the membrane normal. Positive slopes represent transport of positive charge to the extracellular side of the membrane. The negative charge transport at the beginning of the photocycle is small compared to the positive charge displacement during the photocycle. At the end of the photocycle the slow negative charge displacement with a time constant τ_6 can be seen more clearly than in Fig. 2a.

The traces of the electric signals could be approximated by a sum of five exponential functions (Table 1). The first rate corresponds to the response of the measuring circuit and to the $K \rightarrow L$ decay (3 μs). To obtain the charge displacement the amplitudes were converted to the corresponding amplitudes of the integral (Table 2).

In contrast to the absorption changes in the visible and infrared region where an almost unlimited set of signals is available; the photocurrent delivers only one trace for the evaluation of the data. This leads to uncertainties in the fitting procedure because the estimated rates and the estimators for the amplitudes depend on each other, i.e. they are statistically highly correlated and this may cause a high standard deviation.

In the 10 to 500 microsecond range, where three exponential terms are expected (Xie et al. 1987) only two are necessary to describe the data. In the five millisecond range two terms corresponding to the *M*- and *O*-decay are expected. However, if the approximation was started with two initial values in this range, the rates converged with large corresponding amplitudes of opposite sign, thus resulting in a single exponential solution.

The reaction with the longest half time of about 10 ms (τ_6) has very low amplitudes so that its standard deviation is large. However, this additional component is necessary to describe the whole reaction cycle appropriately. Interestingly, the photocurrent signal reverses its sign such that the charge movement is opposite to the general direction of the proton transfer.

Both sets of data, electric and optical signals, were also evaluated together. The data could be approximated with the same rate constants without any further normalization, because the data sets are scaled by their weights. The sum of the weighted squared residuals of each single measurement is compared with the one resulting from fitting the electric and optical data separately. There is no evidence that one set of data dominates the other because the sums of weighted squares are of comparable size. In

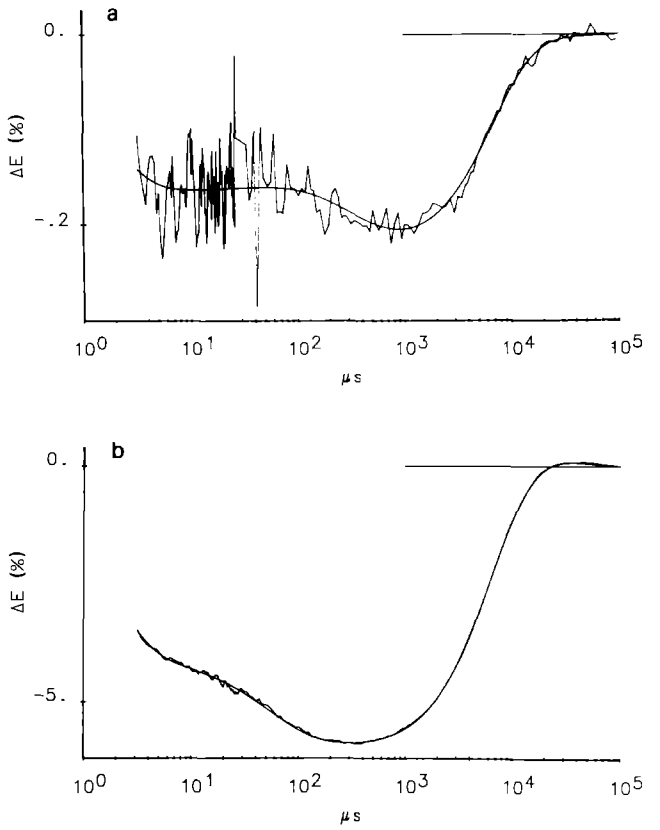

Fig. 3a, b. Time course of infrared absorbance changes of bR after excitation measured at **a** 1800 cm^{-1} and **b** 1525 cm^{-1}. The contineous line represents the fit using the sum of exponential given in Table 1 (Vis_{IR}) and the corresponding amplitudes for **a** 1800 cm^{-1} and **b** 1525 cm^{-1}. The measurements were done on a bR-film as described in Materials and methods

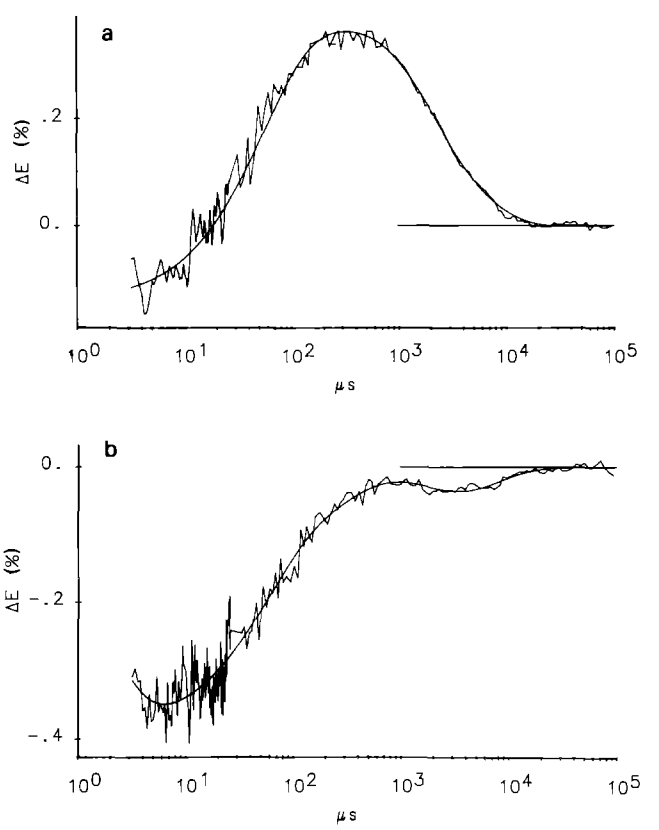

Fig. 4a, b. Time course of infrared absorbance changes of bR after excitation measured at **a** 1765 cm^{-1} and **b** 1740 cm^{-1}. The contineous line represents the fit using the sum of exponential given in Table 1 (Vis_{IR}) and the corresponding amplitudes for **a** 1765 cm^{-1} and **b** 1740 cm^{-1}. Same sample as in Fig. 3

Table 1, the results of the combined evaluations [Vis + El] are given. It should be noted that the two positive amplitudes of the electric signals corresponding to τ_4 and τ_5 are highly correlated. Therefore, only their sum is well defined.

Visible and infrared measurements. In a second set of experiments the photocycle kinetics were determined in the IR region. As representative examples the traces of the absorbance changes at 1800 cm^{-1}, 1525 cm^{-1}, 1765 cm^{-1}, and 1740 cm^{-1} are shown in Figs. 3 and 4. These wavenumbers are characteristic for protonation changes of internal aspartic acids (1765 cm^{-1}, 1740 cm^{-1}) (Engelhard et al. 1985; Eisenstein et al. 1987) and for differences of the chromophore double bond vibration (1525 cm^{-1}). At 1800 cm^{-1}, a wavenumber belonging to a region in which bands from a membrane protein such as bR are absent, absorption changes are clearly visible (Fig. 3a). The corresponding kinetic constants are comparable to τ_3, τ_4, and τ_5 obtained from the other IR signals. This signal could be due to a polarization band caused by hydrogen bonded networks (Brzezinski et al. 1987 and literature therein). However, it should be noted that pH changes of the aqueous phase could also contribute to this signal. The significance of this signal will be discussed below.

In addition to these spectral data, the infrared absorbance changes were monitored at 15 other wavenumbers which cover the area of protonated carboxylic acid vibrations between 1770 cm^{-1} and 1727 cm^{-1}, the amide I mode at 1660 cm^{-1} and 1610 cm^{-1}, and the chromophore vibrations at 1525 cm^{-1}.

All IR data can be approximated with five exponentials [IR] similar to those obtained from the same sample in the visible range [Vis_{IR}] (Table 1). A comparison with the parameters from photocurrent [El] and photocycle [Vis_{IR}] displays almost identical half-lifes (Table 1).

It should be emphasized that τ_6 is only detectable in the measurements at 1525 cm^{-1} and 1660 cm^{-1}. The corresponding amplitude is quite low and its sign is opposite to that of the first part of the signal (Fig. 3b).

B. Amplitude spectra of the protonation changes of internal Asp residues

The fitting procedure provides not only the rates but also the corresponding amplitudes. In Figs. 5 and 6 the amplitude spectra of τ_2, τ_3, τ_4, and τ_5 between 1725 cm^{-1} and 1770 cm^{-1} are plotted. The rate with a half-life time of τ_2 can be correlated with the $L \rightarrow M$ transition. Negative signals can be interpreted as protonation

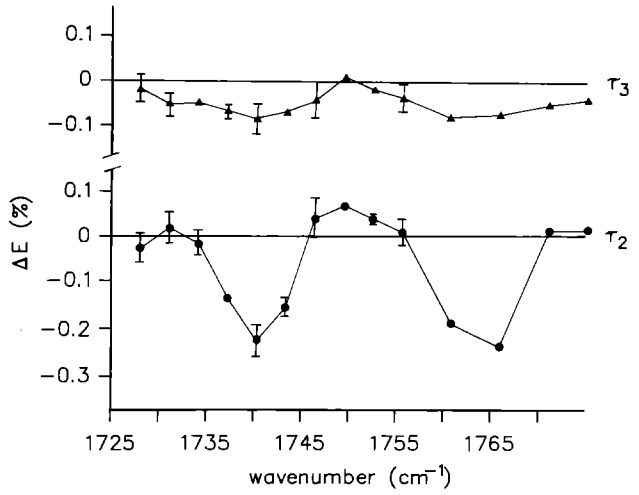

Fig. 5. Amplitude spectra in the infrared region of protonated carboxyl-groups corresponding to the first two rate constants with half times τ_2 and τ_3

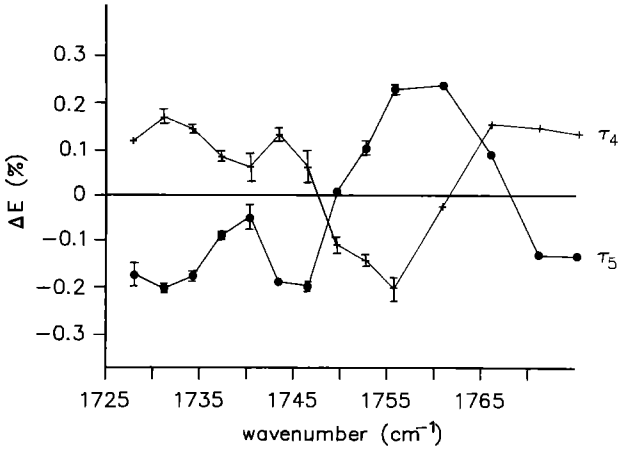

Fig. 6. Amplitude spectra in the infrared region of protonated carboxyl-groups corresponding to the two rate constants with life times τ_4 and τ_5

[$-COO^- \rightarrow -COOH$] and/or environmental changes of a protonated carboxyl group. The two minima at 1740 cm^{-1} and 1765 cm^{-1} were originally interpreted as the protonation of at least two internal Asp residues (Engelhard et al. 1985; Eisenstein et al. 1987). However, recent results using mutant bR's proved that the signal at 1740 cm^{-1} is composed of two differential bands from the protonated Asp115 and Asp96 (Gerwert et al. 1989). The amplitudes of τ_3 have the same general features but with much lower intensities. It is not clear to which transition of the photocycle this rate can be attributed.

The other two rate constants τ_4 and τ_5 describe the decay of *M* and the reformation of bR (Fig. 6). τ_4 has a minimum at 1755 cm^{-1} and a broad band with two small maxima at 1731 cm^{-1} and 1743 cm^{-1}. The amplitudes of τ_5 result in an almost identical spectrum but with an opposite sign. The maximum around 1760 cm^{-1} is now broader and may represent two different chemical groups. It is noteworthy that the amplitudes at wavenumbers above 1770 cm^{-1} do not return to zero, a result which was already described for the 1800 cm^{-1} vibration (see above).

Discussion

The excitation of the retinal chromophore by light evokes specific reactions such as isomerization of the chromophore, deprotonation of the Schiff base and protonation changes at Asp residues. These chromophore and protein reactions can be divided schematically into three parts: The first fast energy requiring events include the isomerization of retinal. This is followed by the deprotonation of the Schiff base and the ejection of a proton to the extracellular side of the membrane. The third, slower part involves the reprotonation of the Schiff base, the reisomerization of retinal, and the uptake of a proton from the cytoplasm which is a passive process, the rate limiting step of which is only determined by the reprotonation of the Schiff base (Butt et al. 1989a). In the experiments presented here, these cyclic events were analyzed using different monitoring functions (reporter groups) which reflect reactions of the protein, the chromophore and charge movement.

The discussion of these results will be subdivided into four parts. In the first section general aspects of the interpretation of the data are presented. The kinetic parameters obtained by the different methods are evaluated subsequently before the individual rate constants are related to photocycle intermediates. The results are then discussed in terms of mechanistic aspects of the intramolecular proton transfer.

Data evaluation

The data obtained could be approximated with a small statistical error using five to six exponentials. This approach assumes that the reactions occur between well defined intermediates and not between populations of closely related species. This latter presumption would result in distributed kinetics and would require a fitting procedure based on power law techniques. This evaluation technique has already been applied to the photovoltage signals of bR by Holz et al. (1988). In the case of the absorption changes in the visible range a model of conformational substates has not yet been rigorously tested. However, discrete first order processes seem to be sufficient to describe the data if branching and back reactions are introduced (e.g. Maurer et al. 1987a, b; Kouyama et al. 1988; Chernavskii et al. 1989; Váró and Lanyi 1990). To allow a comparison with data from the literature in the present study, a sum of first order exponentials is used to evaluate the time course of the reaction cycle.

It is important to note that to derive the intrinsic molecular constants from the fitted kinetics and amplitudes, a specific model has to be applied. Therefore, the calculated values are dependent on the particular model used and without special assumptions no difference- and absolute spectra, e.g. the spectrum of the *N*-intermediate or the corresponding IR difference spectrum, can be obtained.

The simultaneous evaluation of signals of such different quality as IR-, visible-, and photoelectric signals poses some difficulties. For example, a combined analysis of the

kinetic profiles one of which has a high signal to noise ratio (s/n) (e.g. the photocurrent Fig. 2) while the other has a lower s/n (e.g. absorption signal, Fig. 1), will be dominated by the exponentials of the former signal, so that it would be difficult to detect different kinetic processes. The problem was overcome by a weight function which was calculated from the baseline noise or from sets of repeated measurements (see Müller and Plesser 1991 for details).

Another problem arises from the fact that highly correlated exponentials do not give unique solutions. A set of the corresponding kinetic constants will fall within the same statistical confidence limit. If, for example, the fitting procedure is done using the exponential decay measured at two different wavelengths the area of possible solutions becomes smaller. A set of five wavelengths overlapping the absorption band of bR and the *M* and *O* intermediates will suffice to describe the photocycle of unmodified bR (K.-H. Müller, unpublished result).

It should be mentioned that the method used here and described in detail in the accompanying paper (Müller and Plesser 1991) cannot provide an unequivocal proof for a molecular connection of processes observed by different monitors such as, for example, charges and chromophore. This is also true for the case of similar kinetic constants. Additional evidence from biochemical and/or biophysical observations must complement the conclusions. It is also important to note that not all kinetic constants observed have to be monitored by all reporter groups. For example, the amplitude of the time constant τ_5 is zero at 1749 cm^{-1} (for other examples, see Figs. 5 and 6).

Kinetic description of the reaction cycle

The methods presented here are able to monitor reactions at the level of the chromophore, charge displacements, protonation changes of aspartic acids, as well as movements of the peptide backbone. Some signals obtained by the different methods describe the same molecular event. For example, the IR band at 1525 cm^{-1} is characteristic of the conjugated double bonds of the retinal chromophore which can also be analyzed in the visible range. The charge transfer measured by the photocurrent is partly reflected by the deprotonation and protonation of the carboxyl groups of Asp residues.

If the reactions observed have the same origin the corresponding kinetic constants should be identical. On the other hand, this coupling is not generally expected for, for example, the isomerization of the retinal and some distant charge displacements. However, a comparison of the data of Table 1 reveals that all reactions analyzed can be described by the same exponentials.

The observation that the determined rates are identical within the limits of error could be coincidental as already indicated above, although this seems to be rather unlikely. One would expect different molecular events such as charge displacement, chromophore reactions, and protein-backbone movement not to be in exactly the same time intervals. Two other explanations might account for these results. The retinal chromophore could function as an internal monitor which not only detects motions of molecular groups and charges and/or dipoles in its close vicinity but is also sensitive to more distant events. Another explanation for the synchronous reactions could also be found in the assumption that the intramolecular proton transfer is regulated by principal rate determining steps ruling all other transitions. These steps could be the deprotonation and reprotonation of the Schiff base, the 13-*cis* → 13-*trans* isomerization of retinal, conformational changes of the peptide backbone, and/or the protonation and deprotonation of carboxylic groups.

The finding that the data from infrared and photocurrent do not provide additional information on rates connected to the proton transfer – i.e. that only five rates are necessary to describe the thermal reactions from *L* back to the bR resting state – renders it more difficult to deduce a mechanism of the reaction cycle. As already mentioned above, the photocycle cannot be described by an unidirectional unbranched scheme (e.g. Maurer et al. 1987b; Kouyama et al. 1988; Chernavskii et al. 1989; Váró and Lanyi 1990). For example, the accumulated evidence seems to indicate that the *M* decay is characterized by an equilibrium between the intermediates *M* and *N* and between *N* and *O* (Kouyama et al. 1988; Chernavskii et al. 1989) (see also Diller et al. 1988 and Butt et al. 1989a). Applying these models, the rates determined in this study can only be considered as apparent kinetic constants composed of the intrinsic rates. It then follows that the amplitude spectra (Figs. 5–7) are not reflecting a unidirectional transition and can therefore be quite different from true difference spectra.

However, even in the case where the correct model is not known, information might be gained from the kinetic constants and the amplitude spectra. For example, a particular transition in a reaction sequence might make an essential contribution to an apparent rate. This can be assumed if the exponentials are separated well in time, such as, for example, τ_2 and τ_4. Other information can be

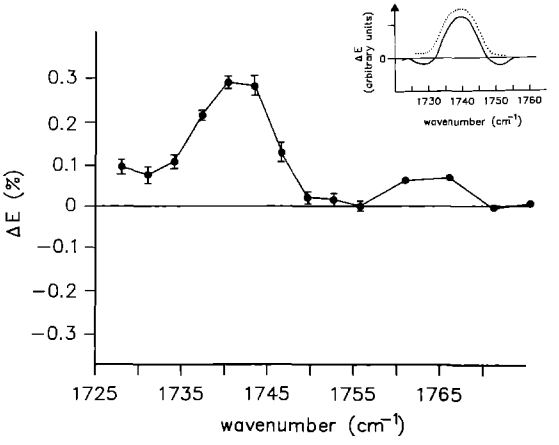

Fig. 7. Infrared bR → *L* difference spectrum of the carboxyl-group region. The data were derived from an extrapolation of the measured amplitude to $t=0$. The insert represents an idealized shape of the difference spectra from steady state measurements at low temperatures and kinetic experiments at room temperature

obtained from amplitude spectra if they are interpreted together with supplementary biochemical data. This will be shown for τ_5 (see below).

Taking these restrictions into account, the determined apparent rate constants and their connection to photocycle intermediates are discussed in the following paragraph.

Apparent rate constants and photocycle intermediates

The five time constants described in this study are similar to those published by Xie et al. (1987), especially if one considers the slow part of the reaction cycle. The apparent rate constants belonging to τ_3 to τ_6 are almost identical to their k_7, k_4, k_3, and k_6, respectively. However, they need two constants with half-life times of 20 µs and 69 µs to adequately fit the first part of the photocycle. These two exponentials could not be verified in this work using the visible, IR, and photocurrent signals. Only one exponential with a half-life time of $\simeq 40$ µs was needed to describe the data. The data are also in agreement with apparent rates determined by Maurer et al. (1987b). In their analysis five exponentials with half lifes of $\tau_1 = 2$ µs, $\tau_2 = 27$ µs, $\tau_3 = 100$ µs, $\tau_4 = 2$ ms, and $\tau_5 = 5$ ms were sufficient to describe the traces of the absorbance changes.

τ_1: The fastest time constant (τ_1) is necessary to describe the data; however, it is not only determined by the photoresponse of bR which falls into the $K \rightarrow L$ transition. Artifacts from the laser-response and the measuring circuit also contribute to this component. Therefore, it is not possible to deduce an amplitude spectrum corresponding to this time constant.

Nevertheless, information about the bR $\rightarrow L$ transition can be gained by extrapolating the amplitudes to $t = 0$. This is shown in Fig. 7. It should be emphasized that this figure does not represent an amplitude spectrum but a difference spectrum between bR and the L-intermediate and can therefore be directly compared to already published infrared difference spectra. A comparison of these difference spectra with those gained from steady state measurements at low temperatures (Engelhard et al. 1985; Eisenstein et al. 1987; Braiman et al. 1988; Gerwert et al. 1989) reveals characteristic differences in the form of this signal which are schematically represented in the insert of Fig. 7. Whereas the difference-band from static measurements at low temperatures has positive features at the edges of the centerband the amplitude of the corresponding spectrum from the kinetic experiments never crosses the base line to give rise to a clear positive band.

Braiman et al. (1988) and Gerwert et al. (1989) assign this band to Asp96 and Asp115. However, they disagree in the interpretation of the underlying molecular reaction. Whereas Braiman et al. (1988) assume a deprotonation of Asp96, this is refuted by Gerwert et al. (1989) who explain these spectral features with environmental changes of the two protonated Asp96 and Asp115. This latter explanation seems to be in good agreement with the spectral form which can be interpreted as two differential bands.

τ_2: The second component τ_2 with a half-time of about 40 µs, which could be determined with sufficient statistical confidence, is well separated by one order of magnitude from the following rate (τ_4). This component has therefore no contributions from the later parts of the photocycle and one can assume that this rate is closely related to the decay of L and the formation of M.

The amplitude spectrum of this rate (Fig. 5) has two minima at 1765 cm^{-1} and 1740 cm^{-1}. The signal at 1765 cm^{-1} was interpreted as the protonation of one internal Asp (Engelhard et al. 1987). On the other hand, the 1740 cm^{-1}-band is composed of the two protonated carboxyl-groups of Asp96 and Asp115 which are undergoing an environmental shift (Gerwert et al. 1989). On the basis of these observations and from data from the literature (Braiman et al. 1988) and own work (F. Siebert et al. unpublished results) it can be stated that Asp85 becomes protonated during the $L \rightarrow M$ transition: The M-intermediate is characterized by three protonated aspartic acid residues.

τ_3: It is not clear how τ_3 can be interpreted. Xie et al. (1987) who first observed this rate do not assign this rate to a specific spectral form. Diller and Stockburger (1988) ascribe a rate constant in the same range as τ_3 to an L-like species originating from a second bR population. Also, inhomogeneities of the bR-samples could be responsible for two rate constants leading from L to M (for a more detailed discussion see below). On the other hand it could also be possible that it belongs to the M decay part of the photocycle and would then be composed of several intrinsic rate constants.

τ_4 and τ_5: τ_4 and τ_5 represent the reactions between the M intermediate and the bR initial state. They are highly correlated (see Müller and Plesser 1991). These exponentials reflect a part of the photocycle whose mechanism is still controversial (e.g. Váró et al. 1990; Váró and Lanyi 1990; Ames and Mathies 1990; Chernavskii et al. 1989). The discussion involves the number of intermediates and the position of these intermediates in the photocycle.

General agreement exists about the requirement for back reactions, and the data presented here are in good agreement with this assumption. However, the fitting of the data to published models did not confirm or refute a particular model (unpublished result). In the following discussion the position of τ_4 and τ_5 in the photocycle will be assessed by the evaluation of the amplitude spectra (Figs. 6, 8) and biochemical data from the literature.

τ_5 shows positive bands at 1765 cm^{-1} and 1755 cm^{-1} which are characteristic for the deprotonation of Asp residues. Since independent evidence suggests that Asp212 and Asp85 are deprotonated in the ground state this rate must be correlated to the reformation of bR (Gerwert et al. 1989; Braiman et al. 1988; Engelhard et al. 1989, 1990; Siebert et al. in preparation): In earlier work using time resolved IR techniques it has been shown that the absorption changes at 1765 cm^{-1} and 1755 cm^{-1} are kinetically different and it was argued that these signals are due to two Asp residues which are deprotonated in the ground state (Siebert et al. 1982; Engelhard et al. 1985). Since the sign of the amplitudes between 1770 cm^{-1} and 1745 cm^{-1} is positive this band is due to a deprotonation and this must necessarily succeed signals which can be explained by a protonation, such as τ_2 and τ_4.

These arguments correlate a substantial portion of τ_5 with the $O \rightarrow$ bR transition and are consistent with most published models which assume an irreversible $O \rightarrow$ bR reaction.

If the different kinetic behavior at 1755 cm^{-1} and 1765 cm^{-1} is due to two aspartic acids it follows also from these conclusions that the O-intermediate is characterized by four protonated carboxyl-groups from Asp85, Asp96, Asp115, and possibly Asp212. However, additional information from bR/M infrared-difference spectra of a mutant of bR in which Asp85 is changed to Glu (Asp85 → Glu) (Braiman et al. 1988) reveals the whole band pattern between 1745 cm^{-1} and 1770 cm^{-1} to be absent. The authors ascribe this signal solely to Asp85. However, as pointed out above this band contains two different kinetic processes at two different spectral positions (1755 cm^{-1} and 1765 cm^{-1}). There are at least three explanations for these discrepancies. It might be possible that two different populations of bR (at least at the stage of the L-intermediate) give rise to the two signals that the mutation not only removes the Asp85 vibration but also shifts the vibrational mode of Asp212, or that this mode is due to Asp96. It should be noted, that Rothschild et al. (1990) ascribe a band at 1738 cm^{-1} to Asp212. This assignment seems to be problematic since it was gained from mutants (Asp212 → Asn, Glu, Ala) whose functional and spectroscopic properties do not resemble the native protein. The assumption proposing different population in the bR resting state was already discussed using independent observations (El-Sayed et al. 1989; Diller and Stockburger 1988). Specific ^{12}C and ^{13}C incorporation into Asp212 should provide a means of deciding between the possibilities and for the unequivocal assignment of the Asp212 carbonyl vibration.

Furthermore, the conclusion that the deprotonation of two Asp residues occurs during the decay of O would raise some difficulties, since one then has to explain which molecular groups are accepting these two protons. The Schiff base is already reprotonated at this stage of the reaction cycle. Another possibility, Asp96, seems to be unlikely because the corresponding signal at 1740 cm^{-1} where the vibrational mode of Asp96 is observed (Braiman et al. 1988; Gerwert et al. 1989) is missing. One possible proton accepting group could be Arg82 which was proposed to be involved in the proton release pathway (e.g. Ames and Mathies 1990).

The question arises of whether the amplitude spectra corresponding to τ_4 and τ_5 provide evidence for a de- and reprotonation of Asp96 after the formation of M, as was proposed by Gerwert et al. (1989). Asp96 absorbs at 1740 cm^{-1} (Braiman et al. 1988; Gerwert et al. 1989), a region where only minor amplitudes are observed (Figs. 6 and 8). This indicates that Asp96 is protonated in M as well as in O. A transient deprotonation including N cannot, however, be excluded if τ_4 represents an apparent rate with only minor contributions of N.

The amplitudes of the photoelectric signal and the amide I vibration at 1660 cm^{-1} change primarily with the rates corresponding to τ_2 and τ_5 (Table 2). Obviously the protein undergoes a conformational rearrangement, thereby facilitating the movement of charges. Fodor et al.

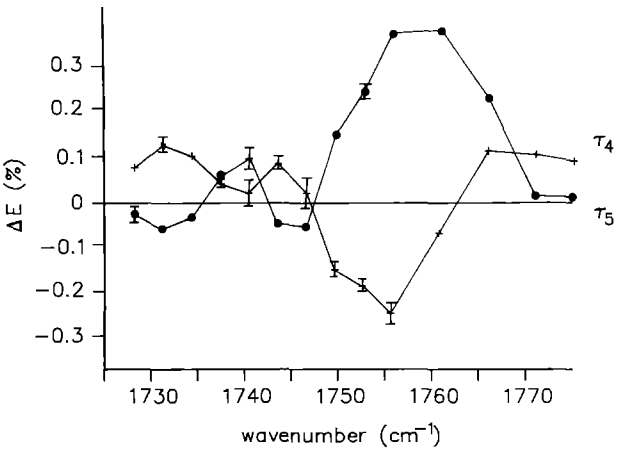

Fig. 8. Amplitude spectra in the infrared region of protonated carboxyl-groups corresponding to τ_4 and τ_5. Same as in Fig. 6, however, substracted with the corresponding amplitudes measured at 1800 cm^{-1}

(1988) proposed a mechanism of the proton pump in which the conformation of the protein is responsible for the vectorial transfer of the proton. In their model the main protein switch should be observed in the range of the amide vibrations during the $L \rightarrow M$ and $N \rightarrow O$ transition. In this study the major effects are observed with τ_2 and τ_5. Whereas τ_2, in agreement with these authors and with data from the literature (Engelhard et al. 1985; Braiman et al. 1988) probably correspond to the $L \rightarrow M$ transition, τ_5 seems to be mainly composed of the $O \rightarrow$ bR reaction. Apparently, a major conformational change of the protein occurs in the last step of the photocycle.

τ_6: The slowest component of the photocycle (τ_6) was first observed by Gillbro (1978). It is not only found in the visible range but can also be recognized in the signal of the 1525 cm^{-1} band. This was to be expected since this band represents chromophore vibrations. But, interestingly, the photocurrent also has a component with this time constant. The sign of the amplitude is opposite to the proton transfer as if the system overshoots and has to relax back to the ground state. The intermediate connected with this time constant must closely resemble the bR-resting state. Because all kinetic data were obtained from light adapted samples it seems unlikely that this time constant belongs to the 13-*cis* photocycle.

General conclusions

The signal at 1800 cm^{-1} with major amplitude changes observed with τ_4 and τ_5 (data not shown) does not originate from a particular molecular group of the protein. However, it might be caused by broad uniform polarization bands. These bands are expected if chains of hydrogen bonds exist (Brzezinski et al. 1987). An alteration of these chains of hydrogen bonds during the photocycle would result in the observed signal at 1800 cm^{-1} extending to higher and lower wavenumbers. Indeed, absorbance changes of similar size have been detected at 1850 cm^{-1}, 1890 cm^{-1}, and 1950 cm^{-1} (F. Siebert, unpublished result). It should be emphasized, however, that

this broad unresolved band might also be explained by transient changes of the pH of the aqueous phase during the photocycle.

Irrespective of its origin, this band could be superimposed on the vibrations of the carboxyl groups and extend to higher, normally empty, frequency ranges. That this might indeed be the case is seen in the amplitude spectra of τ_4 and τ_5 (Fig. 6). The signals never reach the base line, especially at 1770 cm^{-1}, as one would expect. Under the assumption that the broad band extends uniformly from 1800 cm^{-1} to 1728 cm^{-1} the amplitudes of the 1800 cm^{-1} signal can be subtracted from the other signals. This is shown in Fig. 8. The amplitudes at 1770 cm^{-1} approach zero, thus justifying the subtraction procedure.

According to electron microscopy data the position of the Schiff base is close to the middle of the membrane and is connected to the cytoplasmic surface via a narrow channel (Henderson et al. 1990). Only one functional group, Asp96, has so far been identified to be involved in this part of the proton transfer chain. This implies that hydrogen bonded chains are necessary to bridge the exterior with the Schiff base. The observation of the absorption changes at 1800 cm^{-1} might be taken as an indication for the existence of such a hydrogen bonded network which might be confined in the narrow channel proposed by Henderson et al. (1990).

The slow components τ_4 and τ_5 are connected to processes which are determined by the uptake of the proton from the cytoplasm and the reprotonation of the Schiff base (Butt et al. 1989 b). However, as can be deduced from Fig. 6, at least Asp85, which is located on the extracellular side of the retinal-chromophore (Henderson et al. 1990), is still protonated within the lifetime of the *O*-intermediate (see also Table 3). In other words, with τ_4 and τ_5, although correlated to the third part of the reaction cycle – the pick-up of a proton and the reprotonation of the Schiff base – molecular events are occurring which are still connected to the second part, the ejection of a proton to the extracellular medium. This demonstrates not only that reactions can happen simultaneously but that they can also be spatially separated at opposite sides of the retinal chromophore. Obviously, the rate determining steps coordinate events not only in time but also at functionally different parts of the molecule.

The results from the joint analysis of photocurrent signals, visible-, and infrared absorption changes are summarized in Table 3. Evidence was provided that all reactions enabling the intramolecular proton transfer are occurring synchronously. The main conformational transitions are observed simultaneously with the electrical signal and the $L \rightarrow M$ and $O \rightarrow$ bR reactions. Throughout the existence of the *O*-intermediate at least Asp85 is still protonated. Its deprotonation, concomitant with the *O*-decay, might also be reflected in the large amplitude of the electrical signal and the conformational alteration of the protein back-bone.

Table 3. Transient protonation state of internal aspartic acids during the photocycle. *The thickness of the arrows* relate to the apparent amplitudes of the electrical signal

	L ➡	*M* ➡	*O* ➡	bR
Asp115	–COOH	–COOH	–COOH	–COOH
Asp96	–COOH	–COOH	–COOH	–COOH
Asp85	$-COO^-$	–COOH	–COOH	$-COO^-$
AspX[a]	$-COO^-$	$-COO^-$	–COOH	$-COO^-$

[a] In the present work one cannot distinguish between an assignment of this residue to Asp85 or Asp212

Acknowledgements. We thank R. Müller for excellent technical help and K. H. Wüster for the preparation of the purple membrane.

References

Ames JB, Mathies RA (1990) The role of back-reactions and proton uptake during the $N \rightarrow O$ transition in Bacteriorhodopsin's photocycle: A kinetic resonance Raman study. Biochemistry 29:7181–7190

Bagley K, Dollinger G, Eisenstein L, Singh AK, Zimányi L (1982) Fourier transform infrared difference spectroscopy of bacteriorhodopsin and its photoproducts. Proc Natl Acad Sci USA 79:4972–4976

Braiman MS, Mogi T, Marti T, Stern LJ, Khorana HG, Rothschild KJ (1988) Vibrational spectroscopy of bacteriorhodopsin mutants: Light-driven proton transport involves protonation changes of aspartic acid residues 85, 96, and 212. Biochemistry 27:8516–8520

Brzezinksi B, Zundel G, Krämer R (1987) Proton polarizability caused by collective proton motion in intramolecular chains formed by two and three hydrogen bonds. Implications for charge conduction in bacteriorhodopsin. J Phys Chem 91:3077–3080

Butt H-J, Fendler K, Dér A, Bamberg E (1989 a) Temperature jump study of charge translocation during the bacteriorhodopsin photocycle. Biophys J 56:851–859

Butt H-J, Fendler K, Bamberg E, Tittor J, Oesterhelt D (1989 b) Aspartic acids 96 and 85 play a central role in the function of bacteriorhodopsin as a proton pump. EMBO J 8:1657–1663

Chernavskii DS, Chizhov IV, Lozier RH, Murina TM, Prokhorov AM, Zubov BV (1989) Kinetic model of bacteriorhodopsin photocycle: pathway from *M* state to bR. Photochem Photobiol 49:649–653

Dancsházy Zs, Drachev LA, Ormos P, Nagy K, Skulachev VP (1978) Kinetics of the blue light-induced inhibition of photoelectric activity of bacteriorhodopsin

Dancsházy Zs, Govindjee R, Nelson B, Ebrey NT (1986) A new intermediate in the photocycle of bacteriorhodopsin. FEBS Lett 209:44–48

Dér A, Hargittai P, Simon J (1985) Time-resolved photoelectric and absorption signals from oriented purple membrane immobilized in gel. J Biochem Biophys Methods 10:295–300

Diller R, Stockburger M (1988) Kinetic resonance raman studies reveal different conformational states of bacteriorhodopsin. Biochemistry 27:7641–7651

Drachev LA, Kaulen AD, Skulachev VP (1978) Time resolution of intermediate steps in the bacteriorhodopsin-linked electrogenesis. FEBS Lett 87:161–167

Drachev LA, Kaulen AD, Skulachev VP (1984) Correlation of photochemical cycle, H^+ release and uptake, and electric events in bacteriorhodopsin. FEBS Lett. 178:331–335

Drachev LA, Kaulen AD, Skulachev VP, Zorina VV (1986) Protonation of a novel intermediate *P* is involved in the $M \rightarrow$ bR step of the bacteriorhodopsin photocycle. FEBS Lett 209:316–320

Eisenbach M, Weissmann C, Tanny G, Caplan SR (1977) Bacteriorhodopsin-loaded charged synthetic synthetic membranes. FEBS Lett 81:77–80

Eisenstein L, Lin SL, Dollinger G, Odashima K, Ding WD, Nakanishi K (1987) FTIR-difference studies on apoproteins. Protona-

tion states of aspartic and glutamic acid residues during the photocycle of bacteriorhodopsin. J Am Chem Soc 109:6860–6862

El-Sayed MA, Lin CT, Mason WR (1989) Is there an excitonic interaction or antenna system in bacteriorhodopsin. Proc Natl Acad Sci USA 86:5376–5379

Engelhard M, Gerwert K, Hess B, Kreutz W, Siebert F (1985) Light-driven protonation changes of internal aspartic acids of bacteriorhodopsin: An investigation by static and time-resolved infrared difference spectroscopy using [4-^{13}C] aspartic acid labeled purple membrane. Biochemistry 24:400–407

Engelhard M, Hess B, Emeis D, Metz G, Kreutz W, Siebert F (1989) Magic angle sample spinning ^{13}C nuclear magnetic resonance of isotopically labeled bacteriorhodopsin. Biochemistry 28:3967–3975

Engelhard M, Hess B, Metz G, Kreutz W, Siebert F, Soppa J, Oesterhelt D (1990) High resolution ^{13}C-solid state NMR of bacteriorhodopsin: assignment of specific aspartic acids and structural implications of single site mutations. Eur Biophys J 18:17–24

Fahr A, Läuger P, Bamberg E (1981) Photocurrent kinetics of purple membrane sheets bound to planar lipid bilayer membranes. J Membr Biol 60:51–62

Fodor SPA, Ames JB, Gebhard R, van den Berg EMM, Stoeckenius W, Lugtenburg J, Mathies RA (1988) Chromophore structure in bacteriorhodopsin's *N* intermediate: Implications for the proton-pumping mechanism. Biochemistry 27:7097–7101

Gerwert K, Hess B, Soppa J, Oesterhelt D (1989) Role of aspartate-96 in proton translocation by bacteriorhodopsin. Proc Natl Acad Sci USA 86:4943–4947

Gerwert K, Souvignier G, Hess B (1990) Simultaneous monitoring of light-induced changes in protein side-group protonation, chromophore isomerization, and backbone motion of bacteriorhodopsin by time-resolved Fourier-transform infrared spectroscopy. Proc Natl Acad Sci USA 87:9774–9778

Gillbro T (1978) Flash kinetic study of the last steps in the photo-induced reaction cycle of bacteriorhodopsin. Biochim Biophys Acta 504:175–186

Henderson R, Baldwin JM, Ceska TA, Zemlin F, Beckmann E, Downing KH (1990) A model for the structure of bacteriorhodopsin based on high resolution electron cryomicroscopy. J Mol Biol 213:899–929

Herrmann TR, Rayfield GW (1976) A measurement of proton current generated by bacteriorhodopsin in black lipid membranes. Biochim Biophys Acta 43:623–628

Hess B, Kuschmitz D, Engelhard M (1982) Bacteriorhodopsin. In: Martonosi AN (ed) Membranes and transport, vol 2. Plenum Press, New York, pp 309–318

Holz M, Lindau M, Heyn MP (1988) Distributed kinetics of the charge movements in bacteriorhodopsin: evidence for conformational substates. Biophys J 53:623–633

Keszthelyi L (1987) Primary charge motions and light-energy transduction in bacteriorhodopsin. Biophys Chem 29:127–136

Keszthelyi L, Ormos P (1980) Electric signals associated with the photocycle of bacteriorhodopsin. FEBS Lett 109:189–193

Kouyama T, Nasuda-Kouyama A, Ikegami A, Mathew MK, Stoeckenius W (1988) Bacteriorhodopsin photoreaction: Identification of a long-lived intermediate N (P, R350) at high pH and its *M*-like photoproduct. Biochemistry 27:5855–5863

Lozier RH, Bogomolni RA, Stoeckenius W (1975) Bacteriorhodopsin: A light-driven proton pump in Halobacterium halobium. Biophys J 15:955–962

Mäntele W, Siebert F, Kreutz W (1982) Kinetic properties of rhodopsin and bacteriorhodopsin measured by kinetic infrared spectroscopy. Methods Enzymol 88:729–740

Maurer R, Vogel J, Schneider S (1987a) Analysis of flash photolysis data by a global fit with multi-exponentials. I. Determination of the minimal number of intermediates in the photocycle of bacteriorhodopsin by the 'stability criterion'. Photochem Photobiol 46:247–253

Maurer R, Vogel J, Schneider S (1987b) Analysis of flash photolysis data by a global fit with multi-exponentials – II. Determination of consistent natural rate constants and the absorption spectra of the transient species in the bacteriorhodopsin photocycle from measurements at different temperatures. Photochem Photobiol 46:255–262

Mogi T, Stern LJ, Marti T, Chao BH, Khorana HG (1988) Aspartic acid substitutions affect proton translocation by bacteriorhodopsin. Proc Natl Acad Sci USA 85:4148–4152

Müller KH, Plesser T (1991) Variance reduction by simultaneous multi-exponential analysis of data sets from different experiments. Eur Biophys J 19:231–240

Nagle JF, Parodi LA, Lozier RH (1982) Procedure for testing kinetic models of the photocycle of bacteriorhodopsin. Biophys J 38:161–174

Oesterhelt D, Hess B (1973) Reversible photolysis of the purple complex in the purple membrane of Halobacterium halobium. Eur J Biochem 37:316–326

Oesterhelt D, Stoeckenius W (1974) Isolation of the cell membrane of Halobacterium halobium and its fractionation into red and purple membrane. Methods Enzymol 31A:667–678

Oesterhelt D, Tittor J (1989) Two pumps, one principle: light driven ion transport in halobacteria. Trends Biochem Sci 14:57–61

Otto H, Marti T, Holz M, Mogi T, Lindau M, Khorana HG, Heyn MP (1989) Aspartic acid-96 is the internal proton donor in the reprotonation of the Schiff base of bacteriorhodopsin. Proc Natl Acad Sci USA 86:9228–9232

Ovchinnikov YA, Abdualev NG, Modyanov NN (1982) Structural basis of proton-translocating protein function. Ann Rev Biophys Bioeng 11:445–463

Parodi LA, Lozier RH, Bhattacharjee SM, Nagle JF (1984) Testing kinetic models for the bacteriorhodopsin photocycle – II. Inclusion of an *O* to *M* backreaction. Photochem Photobiol 40:501–512

Polland H-J, Franz MA, Zinth W, Kaiser W, Kölling E, Oesterhelt D (1986) Early picosecond events in the photocycle of bacteriorhodopsin. Biophys J 49:651–662

Rothschild KJ, Zagaeski M, Cantore WA (1981) Conformational changes of bacteriorhodopsin detected by fourier transform infrared difference spectroscopy. Biochem Biophys Res Commun 103:483–489

Rothschild KJ, Braiman MS, He Y-W, Marti T, Khorana HG (1990) Vibrational spectroscopy of bacteriorhodopsin mutants. Evidence for the interaction of aspartic acid 212 with tyrosine 185 and possible role in the proton pump mechanism. J Biol Chem 265:16985–16991

Siebert F, Mäntele W, Kreutz W (1982) Evidence for the protonation of two internal carboxylic groups during the photocycle of bacteriorhodopsin. FEBS Lett 141:82–86

Soppa J, Oesterhelt D (1989) Bacteriorhodopsin mutants of Halobacterium sp. GRB. J Biol Chem 264:13043–13048

Stern LJ, Ahl PL, Marti T, Mogi T, Duñach M, Berkowitz S, Rothschild KJ, Khorana HG (1989) Substitution of membrane-embedded aspartic acids in bacteriorhodopsin causes changes in different steps of the photochemical cycle. Biochemistry 28:10035–10042

Stoeckenius W, Bogomolni RA (1982) Bacteriorhodopsin and related pigments of halobacteria. Ann Rev Biochem 52:567–615

Tittor J, Soell C, Oesterhelt D, Butt H-J, Bamberg E (1989) A defective proton pump, point-mutated bacteriorhodopsin Asp96 → Asn is fully reactivated by azide. EMBO J 8:3477–3482

Trissl H-W (1985) I. Primary electrogenic processes in bacteriorhodopsin probed by photoelectric measurements with capacitative metal electrodes. Biochim Biophys Acta 806:124–135

Váró G, Lanyi JK (1990) Pathways of the rise and decay of the *M* photointermediate(s) of bacteriorhodopsin. Biochemistry 29:2241–2250

Váró G, Duschl A, Lanyi JK (1990) Interconversion of the *M*, *N*, and *O* intermediates in the bacteriorhodopsin photocycle. Biochemistry 29:3798–3804

Xie AH, Nagle JF, Lozier RH (1987) Flash spectroscopy of purple membrane. Biophys J 51:627–635